A Mechanistic Derivation of The Monod Equation For Biofilm in Porous Media

by

Huizhi Chen

A thesis
presented to the University of Waterloo
in fulfillment of the
thesis requirement for the degree of
Master of Science
in
Earth Sciences

Waterloo, Ontario, Canada, 2021

AUTHOR'S DECLARATION

I hereby declare that I am the sole author of this thesis. This is a true copy of the thesis, including any required final revisions, as accepted by my examiners.

I understand that my thesis may be made electronically available to the public.

Abstract

A mechanistic derivation of the Monod bioreaction equation is presented. The numerical model developed for this derivation involves four processes. 1)On the pore scale, substrate diffuses from the bulk aqueous phase crossing a diffusion boundary layer to the stationary biofilm. 2) On the biofilm scale, the substrate concentration is uniform in the Extracellular Polymeric Substance (EPS) matrix, which equals to that at the biofilm surface. 3) On the microscale, substrates diffuse from the EPS matrix through the EPS layer towards each spherical bacterial cell. 4) Then substrates transport across the cell membrane and react within the microbe for biological reactions. In this numerical model, the derivation incorporates growth kinetics for the bacterial cells and production kinetics for the EPS. The evolution of biofilms and mass transfer processes are simulated under nutrient-limiting and laminar flow conditions. Model parameter sensitivity is examined using data from Reardon et al. (2000), indicating that the diffusive transport of substrate from the aqueous phase to the biofilm is not the most limiting process.

Acknowledgements

I would like to thank my supervisor, Dr. Andre Unger for his unending patience, constant guidance, and encouragement. I'm very appreciative of this opportunity to conduct a multidisciplinary research project.

I would also like to thank my committee members, Dr. Marios Ioannidis and Dr. Yuri Leonenko for their insights and advice.

Thanks to the financial support provided by NSERC and Chevron Energy Technology Company.

Finally, thanks to my family for urging me on to study hard even they are in China and my roommates for their company and delicious cooking especially during the Covid-19.

Table of Contents

AUTHOR'S DECLARATION ii
Abstract iii
Acknowledgements iv
List of Figures vi
List of Tables vii
Chapter 1 Introduction 1
Chapter 2 Methodology 4
2.1 Model Development 4
2.1.1 Bulk concentration of solutes 6
2.1.2 Mass transfer from bulk solution to the biofilm surface 7
2.1.3 Mass balances of solutes within the biofilm 8
2.1.4 Radial diffusion in the unit cell model 8
2.1.5 Mechanistic derivation of the Monod equation 10
2.1.6 Derivation of the mass transfer coefficient at the biofilm surface 12
2.2 The Solution Algorithm 13
Chapter 3 Parameter Sensitivity Analysis 14
Chapter 4 Discussion and Conclusions 17
Bibliography 18

List of Figures

Figure 1. Pore-scale conceptual model 4
Figure 2. The biofilm structure represented by the effective medium (left). The unit cell model (right). ... 9
Figure 3. Substrate depletion and biomass growth with time ($fD = 2$) 15
Figure 4. Substrate depletion and biomass growth with time ($fD = 1.08$) 16
Figure 5. Substrate depletion and biomass growth with time ($fD = 0.11$) 16

List of Tables

Table 1 Symbols and associated units..... 4
Table 2 Monod coefficients from Reardon and Kapellos. 14

Chapter 1 Introduction

In situ bioremediation of groundwater has been one of the most efficient methods to degrade organic contaminants. As the living microorganisms utilize the organic wastes, which are then transformed into less toxic forms, the bacteria adapt to the local environment and eventually form biofilms on grain surfaces (Vidali, 2001). Biofilm development can be achieved by the proliferation of bacterial cells and the simultaneous formation of biopolymers. As the microorganisms grow due to replication of cells and EPS production, they form a structure consisting of a highly porous EPS matrix containing randomly distributed bacterial cells (Charbonneau et al., 2006). Bacterial cells and their surrounding biofilms have proven to be essential in shaping groundwater ecosystems, especially the interactions between the processes in different phases, and yet they remain seriously understudied (Schmidt et al., 2017).

While the Monod equation has been extensively used to describe microbial growth and substrate consumption, the assumption of free-floating bacterial cells in stirred-tank bioreactors is often inappropriate for attached microbes in porous media with the formation of heterogeneous biofilm.

Kim and Fogler (2000) conducted micromodel experiments to reveal the effects of biomass evolution on permeability under both nutrient-rich and nutrient-depleted conditions. Results suggested that the permeability ratio is a function of the amount and integrity of the biofilm. Leon et al. (2004) and Horn and Hempel (1997) attempted to formulize the dependence of biofilm behaviors on varying hydrodynamic conditions. Wäsche et al. (2002) derived empirical equations to calculate mass transfer at the bulk/biofilm interface, based on the dependence of biofilm density and mass transfer on hydrodynamic conditions and substrate concentration. Their empirical equations are restricted to the flow conditions that are achieved in the tube reactor, and thus are inapplicable to describe mass transfer between the bulk and biofilm at the aquifer scale.

Simoni et al., (2001) investigated the factors that affect mass transfer limited biodegradation for low cell densities, where the immobilized cells are loosely clustered without EPS formation. Their results suggested that the cell-based mass transfer coefficient is proportional to the mass transfer area and is independent of flow velocity. However, the situation for low biomass saturation (i.e., isolated spherical microbes) are different from that for biofilms in porous media, because mass transfer per unit biomass is no longer a constant.

Dykaar et al., (1996) introduced mass transfer coefficient at the bulk/biofilm interface using the film theory and boundary layer theory. They determine the mass transfer coefficient (k_l) as a quotient of the diffusion coefficient (D) through the thickness of the concentration boundary layer (δ).

$$k_l = \frac{D}{\delta}$$

Their derivation for a constant mass transfer coefficient is oversimplified given that it ignores the important influence of substrate consumption within the biofilm on the mass transfer efficiency.

Biofilm structure is largely determined by the substrate concentration gradient at the bulk/biofilm interface. While biofilms intrinsically grow as filamentous porous structures, higher detachment force at the biofilm surface will lead to denser biofilms (Van Loosdrecht et al., 1997). Water content of biofilms reaches 90-99% of the total wet mass and water channels (vasculature) can extend from the top to the bottom of the biofilm. Consequently, the internal mass transport is a combination of convection through pores and water channels and diffusive transport through denser aggregates (Horn & Morgenroth, 2006). The driving force inside the biofilm is the biological activities that consume the substrates. Thus, the diffusional mass transfer of the substrates though the cell-polymer clusters is a potential limiting process. Melo (2005) contended that internal mass transfer rates could be equal to the external mass transfer rates and that the relative effective diffusivity is inversely proportional to the tortuosity of the biofilm matrix.

Experimental results showed that effective diffusivity deceased when the biofilm density increased implying that an increase in biofilm density results in less open volume for substrate diffusion through biofilm (Guimerà et al., 2016). In particular, strong mass transfer limitation in biofilm (determined as the ratio of internal diffusivity of biofilms and in free aqueous media, f_D less than 0.1) was observed only when biofilm density greater than 50 $g\ L^{-1}$ volatile suspended solids (Guimerà et al., 2016). This is in close agreement with findings presented by Torresi et al. (2017). They found the concentrations in the bulk liquid and in the biofilm pore liquid converge when the solid-liquid partitioning equilibrium in the biofilm is reached and concluded that diffusive transport is deceased as biofilm density increased (Torresi et al., 2017). Note that biofilm density is inversely proportional to biofilm porosity,

Quantifying biodegradation rates within biofilms requires specifying the biological reaction rate as well as the substrate transport rate within both the biomass phase and the surrounding aqueous phase. Such model should account for substrate transport in flowing groundwater; mass transfer of substrate between bulk solution and stationary biofilm; and biodegradation in biofilm by biological consumptions (Mendoza-Sanchez and Cunningham, 2012). Comprehensive biofilm models in porous media that include an external flow field were developed for the simulation of biofilm structures and the dynamics of biofilm

activity (Picioreanu et al., 1998; Kapellos et al., 2006; Xavier et al., 2005). All the aforementioned studies lack the mechanistic justification for using the Monod kinetics to describe biofilm growth in porous media, where the biofilm growth is composed of both EPS formation and reproduction of microbes.

The objective of this study is to derive the Monod coefficients μ_{max} and K_s from the transport and reaction equations based on the principles of mass conservation and flux continuity. The bioreaction formulation is modified into a Monod form, thus obtaining a mechanistic derivation for the Monod kinetics. The resulting mass transfer coefficients $k_L\ \alpha$ are dependent on three processes: 1) diffusive transport from the bulk aqueous phase to the biomass phase; 2) transport process from the EPS matrix into the bacterial cells; 3) biological reactions depleting the substrates in the microbe. Conservation of mass and flux continuity are implemented at the interfaces between the three phases.

In the model presented herein, the overall transformation fluxes do not become saturated at concentrations as low as predicted for Monod-type kinetics, because Monod equation is for substrate-limiting growth condition when the population density is low. Therefore, mass transfer limitation offers a justification for the common assumption that biodegradation rates in the subsurface follow first order kinetics in a wide concentration range (Simoni et al., 2001). Biofilm structure is represented by an effective medium (Kapellos et al., 2006) assuming the biofilm matrix exhibits a uniform microbe density and that the growth of biofilm proportionately increases the embedded microbial concentration. The transport processes include: diffusive transport from the bulk solution across the boundary layer to the biofilm surface; and, passive diffusion from the surrounding EPS layer towards the cell membrane. The Monod equations for describing the biofilm growth, which includes reproduction of microbes and formation of EPS, are then substituted into the bioreaction equations which are derived based on the mass conservation of the nutrients between biofilm phase and aqueous phase. The resulting formulation of the mass transfer coefficient thus provides mechanistic basis for the Monod kinetics. The numerical model is anticipated to solve the substrate conversion rate, concentration of EPS, and the microbial concentration, under the given biofilm structure (i.e., density, roughness, and thickness).

Chapter 2 Methodology

2.1 Model Development

Mass transport of the biologically reactive solutes includes advection in the bulk aqueous phase, passive diffusion in the diffusion boundary layer and biological reaction in the biofilm. Mass balances of the substrates between the three regions are governed by the mass continuity equations. Figure 1 shows how the system can be conceptualized to obtain the connection between pore-scale concentration experienced by the biomass and macroscopic concentration obtained from aquifer-scale flow equation (Dykaar and Kitanidis, 1996). The mass transfer limitation between the bulk aqueous phase and biomass phase is lumped in the diffusion boundary layer. Table 1 presents the nomenclature.

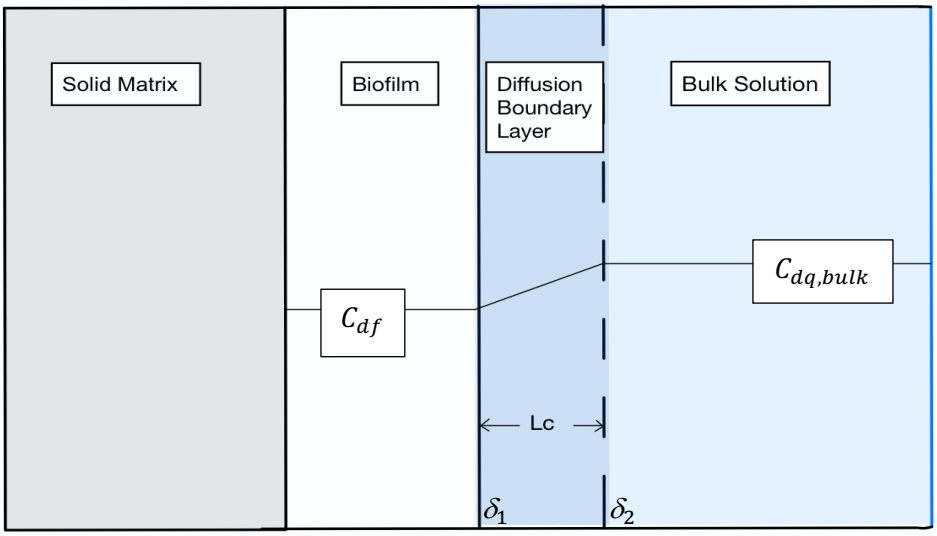

Figure 1. Pore-scale conceptual model

Table 1 Symbols and associated units

A_b	Specific reaction area per microbe $[m^2]$
A_B	Surface area per biofilm $[m^2]$
a	Specific mass transfer area of the biofilm $[m^2 B/m^3 void]$
C_{dq}	Aqueous phase concentration $[kg\ d/m^3\ void]$
$C_{dq,bulk}$	Bulk aqueous phase concentration $[kg\ d/m^3\ void]$
C_{df}	Substrate concentration in the biofilm $[kg\ d/m^3\ ]$
C_{db}	Substrate concentration per unit volume of microbe $[kg\ d/m^3\ b]$

D_{dq}	Aqueous phase molecular diffusion coefficient $[m^2/s]$
D_{df}	Diffusion coefficient of the substrate in the EPS layer $[m^2/s]$
f_D	The ratio of internal diffusivity of biofilms and in free aqueous media $[-]$
J_{dq}	Macroscopic transport rate across surface of biofilm $[kg\ d/m^3\ void/s]$
J_{df}	Mass transport rate in the surrounding EPS layer $[kg\ d/m^3\ b/s]$
J_{db}	Mass transport rate across the cell membrane $[kg\ d/m^3\ b/s]$
K_S	Saturation constant from Monod equation $[kg/m^3]$
$(k_L\ \alpha)$	Mass transfer coefficient $[s^{-1}]$
M_B	Biofilm concentration per unit volume of void $[kg\ B/m^3\ void]$
M_b	Cell concentration per unit volume of void $[kg\ b/m^3\ ]$
M_f	EPS concentration per unit volume of void $[kg\ f/m^3\ ]$
$\mathbb{N}_{db}$	Mass flux of substrate crossing the cell membrane into the interior microbe $[kg\ d/m^2\ b/s]$
$\mathbb{N}_{df}$	Molecular mass flux across the EPS layer towards the microbe surface $[kg\ d/m^2/s]$
$\mathbb{N}_{dq}$	Diffusional mass flux across the surface of the biofilm $[kg\ d/m^2/\ s]$
r	Radius $[m]$
r_b	Radius of a microbe $[m]$
$R_{v,db}$	Macroscopic reaction rate of the biofilm per unit volume of the voids $[kg\ d/m^3\ void/s]$
$R_{B,db}$	Biological consumption rate in the biofilm $[kg\ d/m^3\ /s]$
$\mathbb{R}_{db}$	Microscopic reaction rate per unit volume of microbe $[kg\ d/m^3\ b/s]$
t	Time $[h]$
$\mathbb{v}_{dq}$	Convective velocity of the bulk solution $[m/s]$
$\mathbb{v}_{df}$	Transport velocity across biofilm surface $[m/s]$
V_b	Specific reaction volume per microbe $[m^3]$
Y_{db}	Microbial yield coefficient $[kg\ b/kg\ d]$
ρ_B	Biofilm density $[kg\ B/m^3\ B]$
ρ_b	Microbe density $[kg\ b/m^3\ b]$
k_1	Partitioning coefficient between the aqueous and biomass phases $[-]$
k_2	Partitioning coefficient between the EPS layer and microbes $[-]$
k_d	Specific maintenance rate of the bacterial cells $[s^{-1}]$

μ_{max}	Monod maximum microbial growth rate $[1/s]$
μ_g	Gross specific growth rate of the bacterial cells $[s^{-1}]$
δ_1	Distance from the grain surface to biofilm surface (biofilm thickness) $[m]$
b	Microbe
d	Substrate (electron donor)
f	EPS matrix
B	Biofilm phase

While there are studies about the distribution of diffusion coefficient inside the biofilm matrix, the data from a wide range of experimental systems cannot answer the specific question that depends on the interrelation between biofilm structure and mass transfer (Horn & Morgenroth, 2006). Despite the heterogeneous distribution of the diffusivity within the biofilm matrix, diffusion coefficient is significantly influenced by the biofilm structure (quantified as biofilm density) where it decreases in denser aggregates and increases in looser regions. For biofilms with low cell density, internal transport mechanisms could be the combination of advection and diffusion which will result in $f_D > 1$ (Horn & Morgenroth, 2006). In this presented study, the initial value of biofilm density is $M_B = 0.13[mg/L]$, thus the mass resistance within the biofilm is not significant enough to create concentration gradients and mass transfer is potentially enhanced by the biological consumption.

2.1.1 Bulk concentration of solutes

For macroscopic mass transport, we define the substrate concentration within the aqueous phase q surrounding the biofilm phase B, as $C_{dq,bulk}$ $[kg\ d/m^3\ void]$. $R_{v,db}$ $[kg\ d/m^3\ void/s]$ is the macroscopic reaction rate of the biofilm per unit volume of the voids. Thus, the dynamics of the bulk concentration of solute d can be computed from the mass continuity equation:

$$\frac{\partial C_{dq,bulk}}{\partial t} + \mathbb{v}_{dq} \cdot \nabla C_{dq,bulk} = R_{v,db} \quad (1)$$

where the del operator (∇) is the gradient of a function in Cartesian coordinates. If we assume stationary liquid such that solute transport by convection can be neglected, the rate of change of the bulk concentration $C_{dq,bulk}$ can be simplified to:

$$\frac{\partial C_{dq,bulk}}{\partial t} = R_{v,db} \quad (2)$$

2.1.2 Mass transfer from bulk solution to the biofilm surface

The mass transfer between the macroscopic bulk solution and the pore-scale biofilm can be connected by including a conceptualized diffusion layer, which lumps all the transport limitations between the two phases. Solute concentration near the surface of the biofilm is defined as $C_{dq}\big|_{x=\delta_1}$ $[kg\ d/m^3\ void]$ and diffusion coefficient transverse to the biofilm surface is D_{dq} $[m^2/s]$. Then, the concentration of solute d from the bulk aqueous phase onto the biofilm surface is governed by Fick's law:

$$\frac{\partial C_{dq}}{\partial t} + \mathbb{v}\cdot\nabla C_{dq} = D_{dq}\nabla^2 C_{dq} \tag{3}$$

Assuming that the system is at steady state and solute transport perpendicular to the biofilm surface is solely by diffusion, Equation (3) is simplified to:

$$D_{dq}\nabla^2 C_{dq} = 0 \tag{4}$$

Additional assumptions include: the bulk solution beyond the diffusion boundary layer ($x \geq \delta_2$) is well-mixed with solute concentration $C_{dq,bulk}$; and, the solute concentration at the biofilm surface is $k_1 C_{df}$, where $k_1[-]$ is the partitioning coefficient between the aqueous and biomass phases; and, the solute concentration within the biofilm is uniform throughout its thickness and is C_{df} $[kg\ d/m^3]$. Equation (4) is subject to the following boundary conditions:

$$C_{dq} = C_{dq,bulk}, at\ x = \delta_2 \tag{5}$$

$$C_{dq} = k_1 C_{df}, at\ x = \delta_1 \tag{6}$$

where L_c is the thickness of the diffusion boundary layer:

$$\delta_2 - \delta_1 = L_c \tag{7}$$

Thus, Equation (4) can be solved and the concentration profile within the diffusion boundary layer is:

$$C_{dq} = C_{dq,bulk} + \frac{C_{dq,bulk} - k_1 C_{df}}{L_c}(x - \delta_2) \tag{8}$$

Thus, diffusional mass flux $\mathbb{N}_{dq}[kg\ d/m^2\cdot s]$ at the biofilm surface is:

$$\mathbb{N}_{dq} = D_{dq}\frac{\partial C_{dq}}{\partial x}\Big|_{x=\delta_1} \tag{9}$$

The resulting macroscopic transport rate J_{dq} $[kg\ d/m^3\ void/s]$ is:

$$J_{dq} = \alpha D_{dq}\frac{\partial C_{dq}}{\partial x}\Big|_{x=\delta_1} \tag{10}$$

Where α $[m^2 B/m^3 void]$is the specific mass transfer area of the biofilm:

$$\alpha = \frac{A_B}{V_B} \tag{11}$$

Where $A_B[m^2]$ is the surface area of the biofilm and $V_B[m^3]$ is the volume of the biofilm.

2.1.3 Mass balances of solutes within the biofilm

Assuming the perturbation to the concentration profile within the biofilm due to the radial diffusion towards each individual bacterial cell is not substantial, we assume substrate concentration $C_{df}[kg\ d/m^3]$ is uniform within the biofilm (f) and equals to that at the biofilm/bulk interface (i.e., $x = \delta_1$):

$$C_{df} = \frac{C_{dq}|_{x=\delta_1}}{k_1} \tag{13}$$

Justification for this assumption follows from the channels (vasculature) within the biofilm enabling some degree of convective transport of substrate within the biofilm, where this transport rate is greater than the radial aqueous phase diffusive transport of substrate towards the surface of the microbe.

The rate of change in mass concentration of substrate d with respect to time equals to the biological consumption rate per unit volume of biofilm $R_{B,db}[kg\ d/m^3/s]$ and can be written as:

$$\frac{\partial C_{df}}{\partial t} = R_{B,db} \tag{14}$$

Assuming the mass transfer of substrate between the bulk solution and the biofilm reaches steady state, which means there is no accumulation of substrate at the surface of biofilm or within the biofilm, the mass continuity between the three regions (i.e., bulk solution, surface of biofilm and biofilm) can be governed by the following equations:

$$R_{v,db} = J_{dq} \tag{15}$$

$$J_{dq} = R_{B,db} \tag{16}$$

2.1.4 Radial diffusion in the unit cell model

According to Kapellos et al., (2007), the inhomogeneous biofilm structure is represented by unit cells embedded in an effective medium which has homogeneous properties (e.g., uniform biomass concentration). The unit cell model is comprised of a bacterial cell surrounded by Extracellular Polymeric Substances (EPS). In the vicinity of each microbe (i.e., $r_b \leq r \leq \infty$), substrates diffuse from the surrounding EPS layer towards the cell membrane (Kapellos et al., 2007) (see Figure 2).

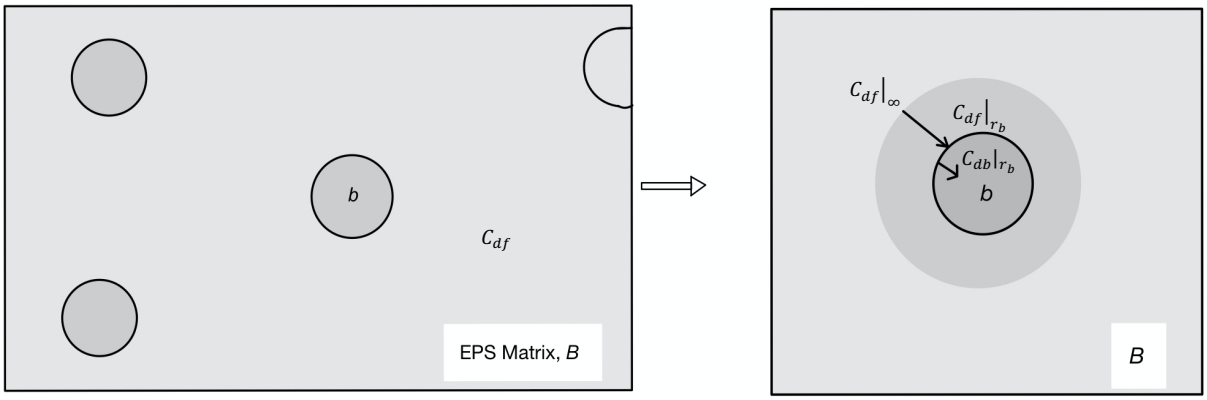

Figure 2. The biofilm structure represented by the effective medium (left). The unit cell model (right).

The rate of change of mass concentration within this surrounding EPS layer is described by:

$$\frac{\partial C_{df}}{\partial t} = -\nabla \cdot \mathbb{N}_{df} \tag{17}$$

where $\mathbb{N}_{df}[kg\ d/m^2 \cdot s]$ is the molecular mass flux. Assume steady state to solve Equation (17):

$$D_{df} \nabla^2 C_{df} = 0 \tag{18}$$

where $D_{df}[m^2/s]$ is the diffusion coefficient of substrate within the EPS layer. Thus, we can solve Equation (18) by writing the equation of radial diffusion from surrounding EPS layer towards the cell membrane:

$$D_{df} \frac{1}{r^2} \frac{\partial}{\partial r} \left(r^2 \frac{\partial C_{df}}{\partial r} \right) = 0 \tag{19}$$

Since the substrate concentration outside the surrounding EPS layer (in the EPS matrix, $r \to \infty$) is assumed to be uniform and equals to $C_{df}\big|_{\infty}$, Equation (19) is subject to the following boundary conditions:

$$C_{df} = C_{df}\big|_{\infty} = \frac{C_{dq}|_{x=\delta_1}}{k_1}, at\ \ r \to \infty \tag{20a}$$

$$C_{df} = C_{df}\big|_{r_b} = k_2 C_{db}|_{r_b}, at\ r = r_b \tag{20b}$$

where $C_{db}[kg\ d/m^3 b]$ is the substrate concentration per unit volume of microbe; and $k_2[-]$ is the partitioning coefficient between the EPS and microbes. Thus, concentration profile at the vicinity of each microbe ($r_b \leq r \leq \infty$) can be written as:

$$C_{df} = \frac{r_b}{r} \left(C_{df}\big|_{\infty} - C_{df}\big|_{r_b} \right) + C_{df}\big|_{\infty} \tag{21}$$

2.1.5 Mechanistic derivation of the Monod equation

The microscopic transport flux $\mathbb{N}_{db}$ $[kg\ d/m^2 b/s]$ describes the mass transport of substrate crossing the cell membrane into the interior microbe:

$$\mathbb{N}_{db} = D_{df} \frac{\partial C_{df}}{\partial r} \tag{22}$$

When this process reaches steady-state condition, the microscopic reaction rate $\mathbb{R}_{db}$ $[kg\ d/m^3/s]$ within the volume of a microbe is equal to the transport flux $\mathbb{N}_{db}$ multiplied by the microbial ratio of the spherical surface area to its volume (i.e., $\frac{A_b}{V_b}$). This steady-state condition implies that the substrate transported across the cell membrane is fully reacted and is not accumulating within the microbe.

$$\because \mathbb{R}_{db} = \frac{A_b}{V_b} \mathbb{N}_{db}|_{r_b} \tag{23}$$

$$\therefore \mathbb{R}_{db} = \frac{4\pi r_b^2}{\frac{4}{3}\pi r_b^3} D_{df} \frac{\partial C_{df}}{\partial r}\Big|_{r_b} \tag{24}$$

Then we define the mass transfer coefficient at the microbial scale as $(k_L\ \alpha)_{\ df}$ $[s^{-1}]$ to quantify the mass transport rate in the surrounding EPS layer J_{df} $[kg\ d/m^3\ b/s]$.

$$J_{df} = (k_L\ \alpha)_{\ df} \left(C_{df}\big|_{\infty} - C_{df}\big|_{r_b} \right) \tag{25}$$

where $k_L = \frac{D_{df}}{r_b}$ and $\alpha = \frac{3}{r_b}$. Similarly, if we assume $C_{db}|_{r_{b,interior}} = 0$, mass transport rate across the cell membrane J_{db} $[kg\ d/m^3\ b/s]$can be written as:

$$J_{db} = (k_L\ \alpha)_{\ db} C_{db}|_{r_b} \tag{26}$$

Applying steady-state condition:

$$\because \mathbb{R}_{db} = J_{df} \tag{27}$$

$$\therefore \mathbb{R}_{db} = (k_L\ \alpha)_{\ df} \left(C_{df}\big|_{\infty} - C_{df}\big|_{r_b} \right) \tag{28}$$

Furthermore, we enforce the mass continuity across the EPS layer by specifying:

$$J_{db} = J_{df} \tag{29}$$

Then by equating eq (26) and (25), we can derive substrate concentration at the cell membrane where $C_{df}\big|_{r_b} = k_2 C_{db}\Big|_{r_b}$:

$$(k_L\ \alpha)_{\ db} C_{db}|_{r_b} = (k_L\ \alpha)_{\ df} \left(C_{df}\big|_{\infty} - C_{df}\big|_{r_b} \right) \tag{30}$$

and rearrange it for the preferred form to solve for the Monod coefficient K_S $[kg/m^3]$:

$$C_{df}\big|_{r_b} = \frac{(C_{df}|_{\infty})^2}{K_s + C_{df}|_{\infty}} \tag{31}$$

$$K_s = \frac{(k_L\ \alpha)_{\ db}}{(k_L\ \alpha)_{\ df}} \frac{C_{df}|_{\infty}}{k_2} \tag{32}$$

$$J_{db} = (k_L\ \alpha)_{\ db} \frac{C_{df}|_{\infty}}{k_2} \frac{C_{df}|_{\infty}}{K_s + C_{df}|_{\infty}} \tag{33}$$

Next, by equating Equation (27) and (29) we can get $\mathbb{R}_{db} = J_{db}$ and write $R_{B,db}$ in terms of $(k_L\ \alpha)_{\ db}$:

$$\mathbb{R}_{db} = (k_L\ \alpha)_{\ db} \frac{C_{df}|_{\infty}}{k_2} \frac{C_{df}|_{\infty}}{K_s + C_{df}|_{\infty}} \tag{34}$$

$$R_{B,db} = \frac{M_b}{\rho_b}\ \mathbb{R}_{db} \tag{35}$$

$$R_{B,db} = \frac{M_b}{\rho_b} (k_L\ \alpha)_{\ db} \frac{C_{df}}{k_2} \frac{C_{df}}{K_s + C_{df}} \tag{36}$$

where M_b is the mass concentration of the cells $[kg\ b/m^3\ ]$ and ρ_b is the cell density $[kg\ b/m^3\ b]$. Then, we can derive the macroscopic reaction rate:

$$\because R_{v,db} = R_{B,db} \tag{37}$$

$$\therefore R_{v,db} = \frac{M_b}{\rho_b} (k_L\ \alpha)_{\ db} \frac{C_{df}}{k_2} \frac{C_{df}}{K_s + C_{df}} \tag{38}$$

Then, substitute Equation (2) $\left(\text{i.e.}, \frac{\partial C_{dq,bulk}}{\partial t} = R_{v,db}\right)$ into eq (38) to solve for the bulk concentration:

$$\frac{\partial C_{dq,bulk}}{\partial t} = -\frac{M_b}{\rho_b} (k_L\ \alpha)_{\ db} \frac{C_{df}}{k_2} \frac{C_{df}}{K_s + C_{df}} \tag{39}$$

The above equations show that the substrate concentration is dependent on the Monod coefficient K_s. Since the biofilm is formed by bacterial cells and EPS, we can write the biofilm concentration $M_B[kg\ B/m^3\ void]$ as:

$$M_B = M_b + M_f \tag{40}$$

Where $\rho_B[kg\ b/m^3\ B]$ is the biofilm density and $M_b[kg\ b/m^3\ void]$ is the cell concentration per unit volume of void; $M_f\ [kg\ f/m^3\ void]$ is the EPS concentration. The Monod equation is written as:

$$\frac{1}{M_b} \frac{dM_b}{dt} = \mu_g \tag{41a}$$

$$\mu_g = \mu_{max} \left(\frac{C_{df}}{K_s + C_{df}} \right) \tag{41b}$$

Where the gross specific growth rate $\mu_g\ [s^{-1}]$ equals to the net growth rate by assuming there is no loss of cell mass; and $\mu_{max}[s^{-1}]$ is the maximum specific growth rate of the bacterial cells. Simultaneously, the cells synthesize EPS with a rate proportional to the growth rate of the bacterial cells:

$$\frac{dM_f}{dt} = Y_{df} \mu_g M_b \tag{42}$$

Where $Y_{df}\ [kg\ f/kg\ b]$ is the EPS-product yield coefficient. The formation rate of the EPS depends on the kinetic parameters $Y_{df}[kg\ f/kg\ b]$ and $\mu_g[s^{-1}]$ which vary with the different bacterial species. Then, the substrate consumption rate $R_{B,db}[kg\ d/m^3/s]$ can be written as:

$$R_{B,db} = \frac{1}{Y_{db}} \mu_g M_b + \frac{1}{Y_{df}} \mu_g M_b \tag{43}$$

Y_{db} $[kg\ b/kg\ d]$ is the cell yield coefficient. Furthermore, by including Equation (14) (i.e., $\frac{\partial C_{df}}{\partial t} = R_{B,db}$) and eq (36), we can write the substrate concentration within the biofilm C_{df} in the Monod formulation as:

$$\frac{dC_{df}}{dt} = -(\frac{1}{Y_{db}} + \frac{1}{Y_{d\pi}})M_b\mu_{max}\left(\frac{C_{df}}{K_s+C_{df}}\right) \quad (44)$$

$$\because \frac{dC_{df}}{dt} = -\frac{M_b}{\rho_b}(k_L\ \alpha)_{\ db}\frac{C_{df}}{k_2}\frac{C_{df}}{K_s+C_{df}} \quad (45)$$

$$\therefore \mu_{max} = \frac{(k_L\ \alpha)_{\ db}C_{df}}{(\frac{1}{Y_{db}}+\frac{1}{Y_{df}})\rho_b} \quad (46)$$

2.1.6 Derivation of the mass transfer coefficient at the biofilm surface

If mass transfer at the biofilm surface ($x = \delta_1$) reaches steady state, the mass balance can be expressed as:

$$\frac{A_B}{V_B}\mathbb{N}_{dq} = R_{B,db} \quad (47)$$

Equation (3) ($i.e.\ D_{dq}\nabla^2 C_{dq} = 0$) can be solved by using the boundary conditions: Equation (5) and (6):

$$C_{dq} = C_{dq,bulk}, at\ x = \delta_2 \quad (5)$$

$$C_{dq} = k_1 C_{df}, at\ x = \delta_1 \quad (6)$$

Thus, Equation (1) can be solved and the concentration profile within the diffusion boundary layer is:

$$C_{dq} = C_{dq,bulk} + \frac{C_{dq,bulk}-k_1C_{df}}{L_c}(x - \delta_2) \quad (48)$$

Substitute Equation (48) into Equation (7) ($i.e.\ \mathbb{N}_{dq} = D_{dq}\frac{\partial C_{dq}}{\partial x}$) to solve for the mass flux in the diffusion boundary layer:

$$\mathbb{N}_{dq} = \frac{D_{dq}}{L_c}(C_{dq,bulk} - k_1C_{df}) \quad (49)$$

Where $k_1C_{df} = C_{dq}\big|_{x=\delta_1}$ is the substrate concentration at the biofilm surface. Then substitute Equation (47) into Equation (49) to obtain the reaction rate:

$$R_{B,db} = \frac{A_B}{V_B}\frac{D_{dq}}{L_c}(C_{dq,bulk} - k_1C_{df}) \quad (50)$$

where $\frac{A_B}{V_B} = \alpha[m^{-1}]$ is the specific area of the biofilm and $\frac{D_{dq}}{L_c} = k_L\ [m/s]$:

$$R_{B,db} = (k_L\alpha)_{dq}(C_{dq,bulk} - k_1C_{df}) \quad (51)$$

Then solve for the reaction rate $R_{B,db}$ by revisiting Equation (14) (i.e. $\frac{\partial C_{df}}{\partial t} = R_{B,db}$) and Equation (44) (i.e. $\frac{dC_{df}}{dt} = -(\frac{1}{Y_{db}} + \frac{1}{Y_{df}})M_b\mu_{max}\left(\frac{C_{df}}{K_s+C_{df}}\right)$) :

$$R_{B,db} = (\frac{1}{Y_{db}} + \frac{1}{Y_{df}})M_b\mu_{max}\left(\frac{C_{df}}{K_s+C_{df}}\right) \quad (52)$$

2.2 The Solution Algorithm

The numerical algorithm is started by solving C_{df} at time-step $n+1$. Based on Equation (44) $\frac{dC_{df}}{dt} = -(\frac{1}{Y_{db}} + \frac{1}{Y_{df}})M_b\mu_{max}\left(\frac{C_{df}}{K_s+C_{df}}\right)$, we can write the expression for ${C_{df}}^{n+1}$:

$${C_{df}}^{n+1} = {C_{df}}^{n} - \Delta t\,(\frac{1}{Y_{db}} + \frac{1}{Y_{df}}){M_b}^{n}\mu_{max}\left(\frac{{C_{df}}^{n}}{K_s+{C_{df}}^{n}}\right) \tag{53}$$

Where $\Delta t = (t^{n+1} - t^{n})$. Next, solve for $C_{dq,bulk}$ by equating Equation (51) and (45):

$$\because (k_L\alpha)_{dq}(C_{dq,bulk} - k_1C_{df}) = \frac{M_b}{\rho_b}(k_L\,\alpha)_{\,db}\frac{C_{df}}{k_2}\frac{C_{df}}{K_s+C_{df}} \tag{54a}$$

$$\therefore C_{dq,bulk} = \frac{\frac{M_b}{\rho_b}(k_L\,\alpha)_{\,db}\frac{C_{df}}{k_2}\frac{C_{df}}{K_s+C_{df}}}{(k_L\alpha)_{dq}} + k_1C_{df} \tag{54b}$$

We assume the partitioning coefficient between the aqueous and biomass phase k_1 is 1. Then including time-step in Equation (54b) and solving for ${C_{dq,bulk}}^{n+1}$:

$${C_{dq,bulk}}^{n+1} = {C_{df}}^{n+1} + \frac{(k_L\,\alpha)_{\,db}{M_b}^{n}\left(\frac{({C_{df}}^{n+1})^2}{K_s+{C_{df}}^{n+1}}\right)}{\rho_b(k_L\alpha)_{dq}} \tag{55}$$

The specific growth rate μ_g at time-step $n+1$ is:

$${\mu_g}^{n+1} = \mu_{max}\left(\frac{{C_{df}}^{n+1}}{K_s+{C_{df}}^{n+1}}\right) \tag{56}$$

Then substitute Equation (56) into Equation (41a) to solve for cell concentration ${M_b}^{n+1}$:

$${M_b}^{n+1} = {M_b}^{n} + \Delta t\,{M_b}^{n}\mu_{max}\left(\frac{{C_{df}}^{n+1}}{K_s+{C_{df}}^{n+1}}\right) \tag{57}$$

Based on Equation (42) we can write the expression for the EPS concentration ${M_f}^{n+1}$:

$${M_f}^{n+1} = {M_f}^{n} + Y_{df}({M_b}^{n+1} - {M_b}^{n}) \tag{58}$$

Thus, the biomass concentration at the next time step ${M_B}^{n+1}$ is:

$${M_B}^{n+1} = {M_b}^{n+1} + {M_f}^{n+1} \tag{59}$$

Chapter 3 Parameter Sensitivity Analysis

In this section, we verify the model through the substrate depletion and biomass growth curves by applying the simulation parameters itemized in Table 2 (Reardon et al., 2000) (Kapellos et al., 2007).

Table 2 Monod coefficients from Reardon and Kapellos.

P.putida F1	Y_{db} $[g\ b/g\ d]$	Y_{df} $[g\ f/g\ b]$	μ_{max} $[h^{-1}]$	K_S $[mg/l]$
Toluene	1.28	1.2	0.86	13.8

Initially, the biomass concentration is so low that bacterial cells do not form clusters and are separated on the grain surfaces (Simoni et al., 2001). Thus, the initial EPS concentration is $M_f = 0\ \left[\frac{mg}{L}\right]$. When the simulation starts, the EPS is synthesized and secreted by the cells with a rate proportional to the growth rate of the cells. The EPS formation rate depends on the EPS yield coefficient Y_{df} and the increasing cell concentration. According to Reardon et al. (2000), the initial condition for bulk concentration of toluene is $C_{dq,bulk} = 39\ [mg/L]$ and the initial microbe population is $M_b = 0.13[mg/L]$. Value of toluene diffusion coefficient in water D_{dq} is $1.2 * 10^{-9}\ [m^2/s]$ (Emanuelsson and Livingston, 2004). Since the bacterial cells are not embedded in the EPS matrix initially, they are exposed in the bulk solution with the initial condition $C_{df} = C_{dq,bulk}$. According to Picioreanu et al., (2000), the specific area of the biofilm α is derived based on the structural parameters of the biofilm (i.e., compactness, area enlargement, roughness), thickness of the biofilm δ_1 is 145 μm, and the thickness of the diffusion boundary layer ranges from 255 to 400 μm. The sensitivity of the model to the presented parameters is examined under three different values of f_D, defined as the ratio of internal diffusivity of biofilms and in free aqueous media ($f_D = D_{df}/D_{dq}$), at 2, 1.08, 0.11 respectively (Melo, 2005).

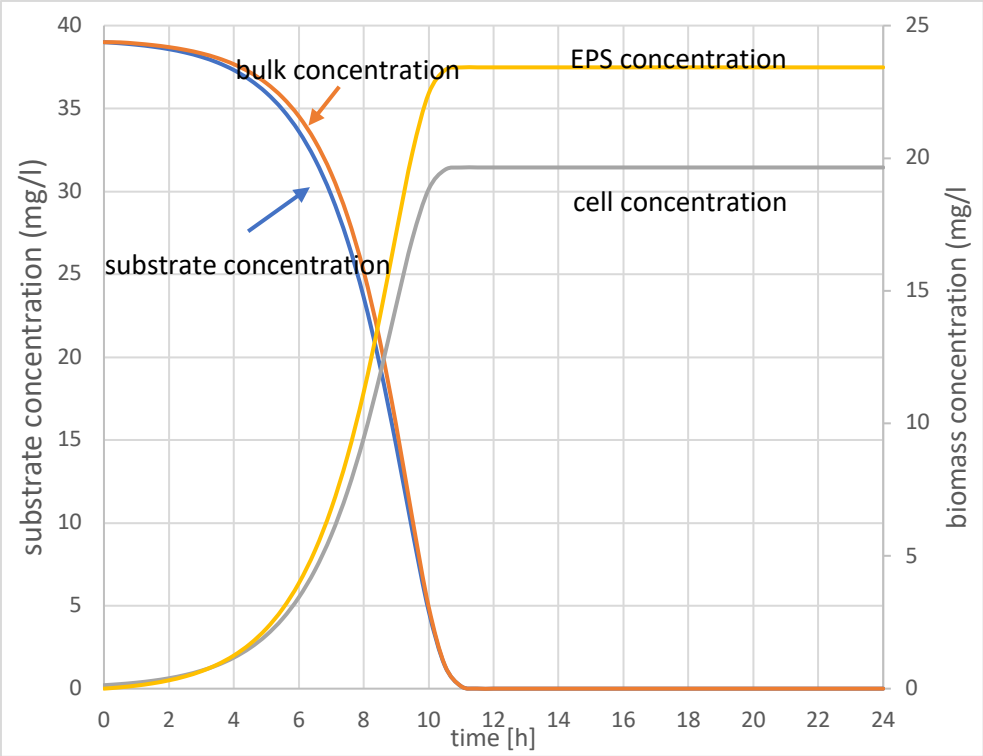

Figure 3. Substrate depletion and biomass growth with time ($\boldsymbol{f_D = 2}$)

As shown in Figure 3, the bacterial cells experience an exponential growth which follows the Monod equation. The EPS concentration starts from zero, then increases proportionally to growth rate of the microbes and exceeds the cell population as the substrates deplete. The concentrations of substrate in the bulk solution and biofilm phase decease during the biomass growth. The aqueous phase concentration is slightly larger than that in the biofilm phase, which forces the diffusive transport of the substrate from the bulk solution to the biofilm.

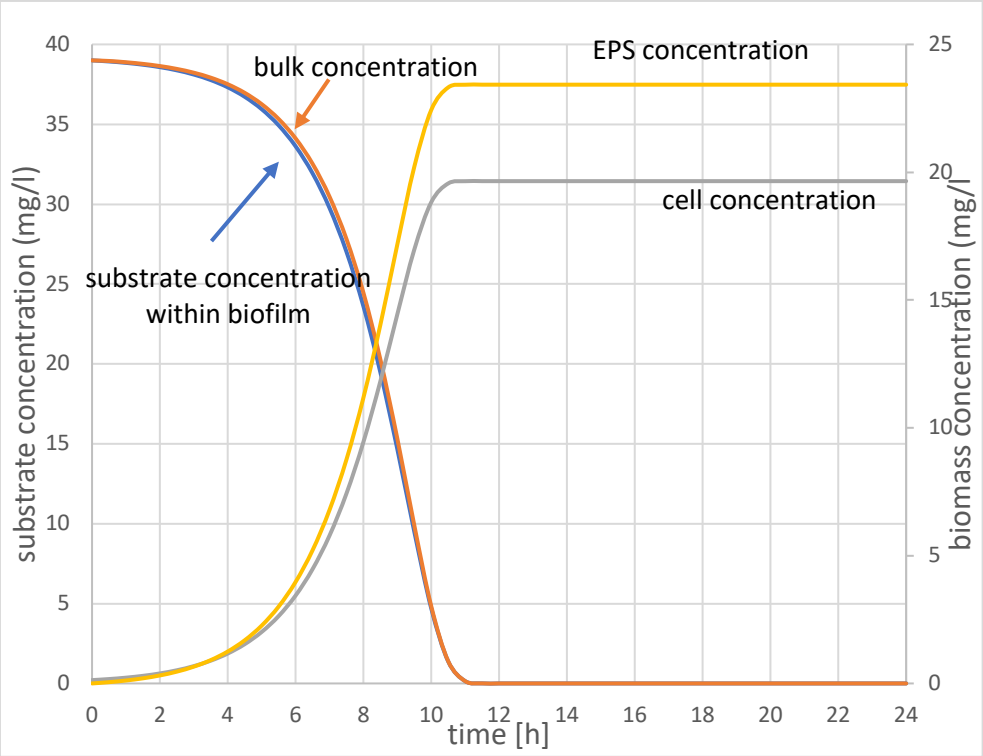

Figure 4. Substrate depletion and biomass growth with time ($f_D = 1.08$)

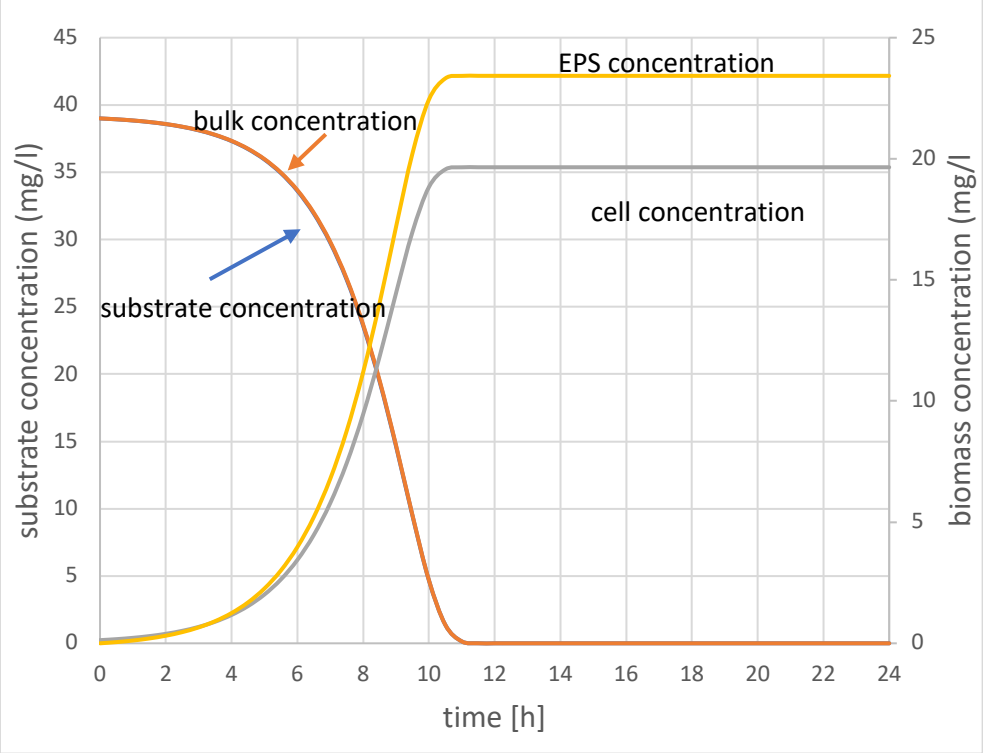

Figure 5. Substrate depletion and biomass growth with time ($f_D = 0.11$)

Chapter 4 Discussion and Conclusions

The basic assumption in this study is that the substrate concentration is uniform in the biofilm matrix. Although we accept heterogeneity of the biofilm structure and the biofilm properties vary with the depth, we assume the internal mass transfer resistance is negligible and consequently, only one diffusion coefficient for substrate within the EPS is used during each simulation. A parameter sensitivity analysis involves toluene depletion, P. putida F1 growth and EPS formation curves, under three different internal mass transport resistance ($f_D = 2, 1.08, 0.11$). Increasing diffusion coefficients within the biofilm (D_{df}) lead to greater substrate concentration difference between bulk solution and biofilm matrix, representing that the mass transfer between the bulk and biofilm phase is not the limiting process ($C_{df}/C_{dq} \approx 1$). According to Gonzo et al. (2014), the relative influence of chemical reaction and diffusion within the biofilm matrix can be expressed as $\sqrt{\frac{{\delta_1}^2 R_{B,db}}{D_{df} C_{dq}}}$ where $R_{B,db}$ follows from Equation (51), which assumes that only diffusive transport exists within the biofilm. While the relative influence of chemical reaction and diffusion increases as the internal diffusion coefficient decreases, the values are all significantly less than one ($\sqrt{\frac{{\delta_1}^2 R_{B,db}}{D_{df} C_{dq}}} \ll 1$) under all three conditions. For biofilms with low cell densities, the internal mass transfer could be enhanced by adventive transport as there is more pore space in the biofilm matrix, which will result in less mass transfer resistance and more uniform distribution of the substrate concentration. Therefore, the assumption that substrate concentration is uniformly distributed within the biofilm matrix is justified.

The mechanistic derivation of the Monod coefficients is performed, and the presented numerical model describes the substrate consumption in biofilm and bulk phases, and the subsequent microbial growth and EPS formation in terms of time. Mass transport is divided into two zones: external bulk solution and internal biofilm matrix. The external mass transport includes the convection of the bulk solution and the transverse diffusion from the bulk into the biofilm. Since there is no substrate consumption in the bulk solution, mass flux of substrates across the biofilm surface must be conserved, which imposes the macroscopic transport rate equals to the overall biological consumption ($J_{dq} = R_{B,db}$).

Bibliography

Charbonneau, A., Novakowski, K., & Ross, N. (2006). The effect of a biofilm on solute diffusion in fractured porous media. Journal of contaminant hydrology, 85(3-4), 212-228.

Dykaar, B. B., & Kitanidis, P. K. (1996). Macrotransport of a biologically reacting solute through porous media. Water Resources Research, 32(2), 307-320.

Emanuelsson, E. A., & Livingston, A. G. (2004). Overcoming oxygen limitations in membrane-attached biofilms—investigation of flux and diffusivity in an anoxic biofilm. Water Research, 38(6), 1530-1541.

Gonzo, E. E., Wuertz, S., & Rajal, V. B. (2014). The continuum heterogeneous biofilm model with multiple limiting substrate Monod kinetics. Biotechnology and bioengineering, 111(11), 2252-2264.

Guimerà, X., Dorado, A. D., Bonsfills, A., Gabriel, G., Gabriel, D., & Gamisans, X. (2016). Dynamic characterization of external and internal mass transport in heterotrophic biofilms from microsensors measurements. Water research, 102, 551-560.

Horn, H., & Hempel, D. C. (1997). Substrate utilization and mass transfer in an autotrophic biofilm system: experimental results and numerical simulation. Biotechnology and bioengineering, 53(4), 363-371.

Horn, H., & Morgenroth, E. (2006). Transport of oxygen, sodium chloride, and sodium nitrate in biofilms. Chemical Engineering Science, 61(5), 1347-1356.

Kapellos, G. E., Alexiou, T. S., & Payatakes, A. C. (2007). A multiscale theoretical model for diffusive mass transfer in cellular biological media. Mathematical biosciences, 210(1), 177-237.

Kapellos, G. E., Alexiou, T. S., & Payatakes, A. C. (2007). Hierarchical simulator of biofilm growth and dynamics in granular porous materials. Advances in Water Resources, 30(6-7), 1648-1667.

Kim, D. S., & Fogler, H. S. (2000). Biomass evolution in porous media and its effects on permeability under starvation conditions. Biotechnology and Bioengineering, 69(1), 47-56.

Leon Ohl, A., Horn, H., & Hempel, D. C. (2004). Behaviour of biofilm systems under varying hydrodynamic conditions. Water Science and Technology, 49(11-12), 345-351.

Melo, L. F. (2005). Biofilm physical structure, internal diffusivity and tortuosity. Water science and Technology, 52(7), 77-84.

Mendoza-Sanchez, I., & Cunningham, J. (2012). Efficient algorithms for modeling the transport and biodegradation of chlorinated ethenes in groundwater. Transport in porous media, 92(1), 165-185.

Picioreanu, C., Van Loosdrecht, M. C., & Heijnen, J. J. (1998). Mathematical modeling of biofilm structure with a hybrid differential-discrete cellular automaton approach. Biotechnology and bioengineering, 58(1), 101-116.

Picioreanu, C., van Loosdrecht, M. C., & Heijnen, J. J. (2000). A theoretical study on the effect of surface roughness on mass transport and transformation in biofilms. Biotechnology and bioengineering, 68(4), 355-369.

Reardon, K. F., Mosteller, D. C., & Bull Rogers, J. D. (2000). Biodegradation kinetics of benzene, toluene, and phenol as single and mixed substrates for Pseudomonas putida F1. Biotechnology and bioengineering, 69(4), 385-400.

Schmidt, S. I., Cuthbert, M. O., & Schwientek, M. (2017). Towards an integrated understanding of how micro scale processes shape groundwater ecosystem functions. Science of the Total Environment, 592, 215-227.

Simoni, S. F., Schäfer, A., Harms, H., & Zehnder, A. J. (2001). Factors affecting mass transfer limited biodegradation in saturated porous media. Journal of Contaminant Hydrology, 50(1-2), 99-120.

Torresi, E., Polesel, F., Bester, K., Christensson, M., Smets, B. F., Trapp, S., ... & Plósz, B. G. (2017). Diffusion and sorption of organic micropollutants in biofilms with varying thicknesses. Water research, 123, 388-400.

Van Loosdrecht, M. C., Picioreanu, C., & Heijnen, J. J. (1997). A more unifying hypothesis for biofilm structures. FEMS Microbiology Ecology, 24(2), 181-183

Vidali, M. (2001). Bioremediation. An overview. Pure and Applied Chemistry, 73(7), 1163-1172. https://doi.org/10.1351/pac200173071163

Wäsche, S., Horn, H., & Hempel, D. C. (2002). Influence of growth conditions on biofilm development and mass transfer at the bulk/biofilm interface. Water Research, 36(19), 4775-4784.

Xavier, J. B., Picioreanu, C., & Van Loosdrecht, M. C. (2005). A framework for multidimensional modelling of activity and structure of multispecies biofilms. Environmental microbiology, 7(8), 1085-1103.